A&A 533, A75 (2011)
DOI: 10.1051/0004-6361/201116590

Astronomy & Astrophysics

Spectroscopic variabilities in λ Pavonis

R. S. Levenhagen[1], N. V. Leister[2], and R. Künzel[3]

[1] Universidade Federal de São Paulo, Depto. Ciências Exatas e da Terra, Rua Prof. Artur Riedel, 275, Jd. Eldorado, CEP 09972-270 Diadema, SP, Brazil
e-mail: ronaldo.levenhagen@gmail.com
[2] Instituto de Astronomia, Geofísica e Ciências Atmosféricas, Universidade de São Paulo, CEP 05508-900 São Paulo, SP, Brazil
[3] Instituto de Física, Universidade de São Paulo, Cidade Universitária, CEP 05508-900 São Paulo, SP, Brazil

Received 26 January 2011 / Accepted 14 July 2011

ABSTRACT

Aims. We investigate the time-varying patterns in line profiles, V/R, and radial velocity of the Be star HD 173948 (λ Pavonis).
Methods. Time series analyses of radial velocity, V/R, and line profiles of He I, Fe II, and Si II were performed with the Cleanest algorithm. An estimate of the stellar rotation frequency was derived from the stellar mass and radius in the Roche limit by adopting an aspect angle i derived from the fittings of non-LTE model spectra affected by rotation. The projected rotation velocity, necessary as input for the spectral synthesis procedure, was evaluated from the Fourier transform of the rotation profiles of all neutral helium lines in the optical range.
Results. Emission episodes in Balmer and He I lines, as well as V/R cyclic variations, are reported for spectra observed in year 1999, followed by a relatively quiescent phase (2000) and then again a new active epoch (2001). From time series analyses of line profiles, radial velocities, and V/R ratios, four signals with high confidence levels are detected: $\nu_1 = 0.17 \pm 0.02$, $\nu_2 = 0.49 \pm 0.05$, $\nu_3 = 0.82 \pm 0.03$, and $\nu_4 = 1.63 \pm 0.04$ c/d. We interpret ν_4 as a non-radial pulsation g-mode, ν_3 as a signal related to the orbital timescale of ejected material, which is near the theoretical rotation frequency 0.81 c/d inferred from the fitting of the models taken into account for gravity darkening. The signals ν_1 and ν_2 are viewed as aliases of ν_3 and ν_4.

Key words. stars: oscillations – stars: fundamental parameters – stars: emission-line, Be – stars: individual: λ Pavonis

1. Introduction

Emission-line B stars (Be stars) present remarkable observational behaviours in all spectral domains. The most outstanding observable characteristic in the visible domain relies on the existence of emission in Balmer lines, often accompanied by emission of singly ionized metals and irregular variabilities of both a spectroscopical and a photometrical nature (Moujtahid et al. 1999). Emission strength variations of spectroscopic lines, wings, and energy distributions in these objects seem to be due to the changing aspects of a circumstellar environment (Vinicius et al. 2006; Zorec et al. 2005; Townsend et al. 2004; Porter & Rivinius 2003). Particularly, the presence of an envelope with temperatures $\sim 10^4$ K seems to be responsible for the optical emission lines as well as for the infrared excess observed.

The mass ejection mechanism and maintainance of the envelope has not yet been fully understood, but in some cases it seems to be related to the presence of non-radial pulsations (NRP), which explain the travelling bumps shown in optical absorption lines. Ando (1983, 1986), Kambe et al. (1993), and Rivinius et al. (1999) have suggested that the coupling of two NRPs modes could supply the amount of energy required to induce discrete ejections. The southern emission-line B star λ Pavonis (HD 173948, HR 7074, HIP 92609, SAO 254393, $B = 4.064$, $V = 4.207$) is a member of the Scorpio-Centaurus association. Its optical spectrum is known to exhibit strong, double-peaked Balmer emissions (Sahade et al. 1988), where these authors mention quiescent and active epochs from 1949 through 1982. Unfortunately, they do not provide spectral samples for Balmer lines, difficulting to constrain its phase transitions and burst ocurrences. Highly-variable Hβ emission episodes are reported by Mennickent (1991) ranging the period 1984–1987. Chen et al. (1989) identified two distinct line profile groups with projected rotational velocities of 170 and 210 km s^{-1} in the IUE spectra, and have interpreted them as distinct extended regions, one in rotation and the other expanding.

In this work, we analyse new spectroscopic data observed both at the ESO's 1.52 m telescope (Chile) and the 1.60 m telescope at the MCT/LNA (Brazil). From these observations, we proceeded with the Fourier analysis of the lpv in He I 4009, 4026, 4121, 4144, 4388, 4471, 4922, 6678 Å, Si II 4131 Å, Mg II 4481 Å, and Fe II 5169 Å lines. From the fitting of non-LTE stellar atmosphere's models to the observed spectroscopic data, we inferred the physical conditions of the photosphere. The polar and equatorial temperatures, superficial gravities and aspect angle i were inferred from the fitting of stellar models distorted by fast rotation (Lovekin et al. 2006; von Zeipel 1924a,b). The bolometric luminosity ($\log L/L_\odot$), stellar mass ($M/M_\odot$), and logarithmic age ($\log \tau$) were derived from interpolations in the tabulated evolutionary tracks of non-rotating stars by Schaller et al. (1992). From the spectroscopic data set, we determined the frequency signals associated to line profile variations (lpv), radial velocity, and V/R, measured from He I, Fe II, and Si II line profiles. Some rapid variabilities have been reported in the past years (Koen & Eyer 2002; Hubert & Floquet 1998) without further detailed studies. Even the binarity scenario has been proposed as a possible mechanism, as proposed by Groh et al. (2007) based on the observations in the X-ray range done by the Einstein Observatory, which pointed to an X-ray source associated to this object.

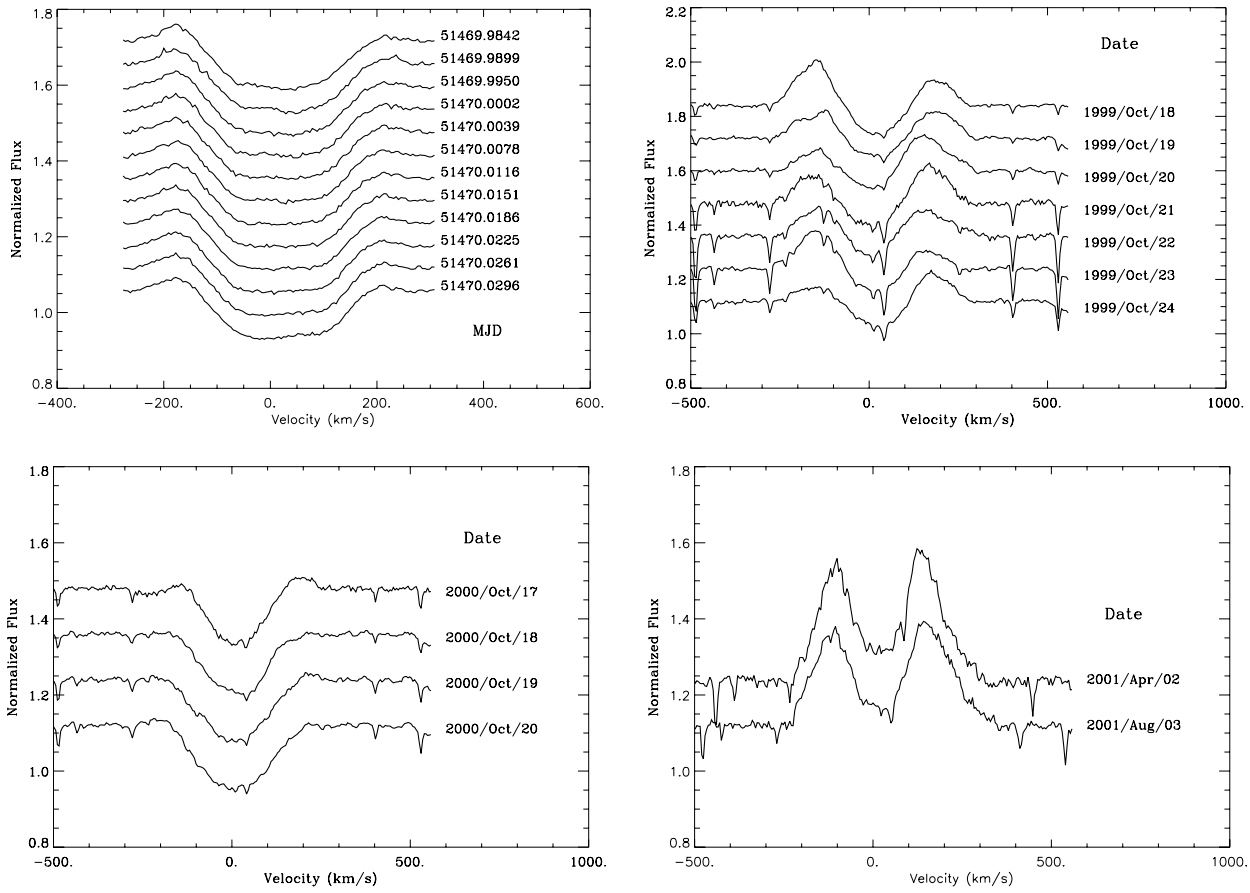

Fig. 1. Observed spectra of λ Pavonis: (*upper left*) He I 6678 Å line profiles concerning to 1999 Oct. 18; (*upper right*) Hα profiles of 1999 observational season, exhibiting V/R rapid variability; (*lower left*) Hα profiles of 2000 observational season, showing an almost quiescent phase; (*lower right*) Hα profiles of 2001, with increasing line activity.

2. Observations

A total of 107 high-resolution and signal-to-noise spectroscopic observations (see Fig. 1 and Table 1) were carried out in the Southern Hemisphere both with FEROS spectrograph associated to the 1.52 m telescope at ESO/La Silla in Chile (observations made with Brazilian time, through CNPq grant No. 1998/10138-8) and with Coudé spectrograph at the 1.60 m telescope of MCT/LNA (Brazil). ESO's spectra were taken with spectral coverage of 3560−9200 Å, with typical $S/N \sim 300$ and a reciprocal dispersion of 0.09 Å/pixel, concerning the He I 4471 Å line. LNA's spectra were gathered with a WI101 CCD camera, from 4279 Å to 4720 Å with reciprocal dispersion of 0.43 Å/pixel (at 4471 Å) using a 600 groove mm^{-1} grating blazed at 4500 Å in first order and a typical $S/N \sim 300$. The images were processed in the same way, basically starting with bias and overscan subtraction, followed by the division of the stellar spectra by an average flat-field exposure, compiled from all the flat fields taken during the night, and finally wavelength-calibrated with Th-Ar lamp spectra. Standard stars of rotation velocity and flux were also observed. All this data reduction was accomplished using the IRAF[1] package.

[1] IRAF is distributed by the National Optical Astronomy Observatories, which is operated by the Association of Universities for Research in Astronomy (AURA), Inc., under cooperative agreement with the National Science Foundation.

3. Photospheric parameters from the spectra

The physical parameters related to the photosphere of λ Pavonis (effective temperature $T_{\rm eff}$, superficial gravity log g, and projected rotation velocity $V \sin i$) are derived through the fitting of non-LTE spectra constrained on the initial ($T_{\rm eff}$, log g, $V \sin i$) parameters, where the initial ($T_{\rm eff}$, log g) come from the fitting of theoretical continuum fluxes to the photometric indices of λ Pavonis given by Johnson & Mitchell (1975). A detailed line fitting procedure is performed with non-LTE profiles synthesized with the SYNSPEC fortran code (Hubeny et al. 1994) in the spectral range 4000 to 5000 Å from plane-parallel, non-LTE atmosphere models computed with TLUSTY code (Hubeny 1988).

The input atomic species adopted in the synthesis procedure were compiled with energy levels, line oscillator strengths, and photoionization cross sections extracted from TOPBASE (Cunto et al. 1993) and updated by the more accurate experimental energy levels from the Atomic and Spectroscopic Database at NIST whenever available (Martin et al. 1999). The model atoms are listed in Table 2. The spectrum-fitting procedure was performed with the downhill simplex algorithm (Nelder & Mead 1965) around the starting ($T_{\rm eff}$, log g, $V \sin i$) values and allowed for both changes in the chemical composition and microturbulence. Solar abundance references were taken from Asplund et al. (2005). Abundances estimates of helium and magnesium were retrieved by seeking microturbulences for which the

Table 1. Log of spectroscopic observations on λ Pavonis.

Date	Telescope	Wavelength range (Å)	Number of spectra	MJD span
1999 Oct. 18	ESO 1.52 m	3560–9200	12	51 469.9842–51 470.0296
1999 Oct. 19	ESO 1.52 m	3560–9200	13	51 471.0214–51 472.0434
1999 Oct. 21	ESO 1.52 m	3560–9200	13	51 472.9886–51 473.0464
1999 Oct. 22	ESO 1.52 m	3560–9200	13	51 473.9794–51 474.0431
1999 Oct. 23	ESO 1.52 m	3560–9200	6	51 474.9849–51 475.1140
1999 Oct. 24	ESO 1.52 m	3560–9200	10	51 476.0000–51 476.1101
2000 Oct. 17	ESO 1.52 m	3560–9200	2	51 835.0303–51 835.0335
2000 Oct. 18	ESO 1.52 m	3560–9200	1	51 836.0288
2000 Oct. 19	ESO 1.52 m	3560–9200	1	51 837.0289
2000 Oct. 20	ESO 1.52 m	3560–9200	1	51 838.0575
2001 Apr. 02	ESO 1.52 m	3560–9200	3	52 002.3689–52 002.4015
2001 Jun. 29	MCT/LNA 1.60 m	4279–4720	6	52 090.7958–52 090.8384
2001 Jun. 30	MCT/LNA 1.60 m	4279–4720	6	52 091.7916–52 091.8397
2001 Aug. 03	ESO 1.52 m	3560–9200	3	52 125.1852–52 125.1958

Table 2. Number of energy levels and radiative transitions adopted in synthesis procedures.

Ion	E_i	Transitions	Ion	E_i	Transitions
He I	50	280	Mg I	50	215
C I	80	716	Mg II	30	176
C II	40	189	Al II	80	528
C III	34	105	Al III	19	60
N I	80	531	Si I	50	186
N II	50	279	Si II	40	206
N III	34	128	Si III	70	414
O I	50	211	S I	50	206
O II	70	468	S II	23	43
O III	28	67	S III	27	55
Ne II	50	258			

abundance values are nearly independent of the line equivalent widths, which demands the knowledge of oscillator strengths, energies for each level, van der Waals damping constants, and Stark broadening parameters for each transition. The other elements were kept with their solar abundances values during synthesis procedure, since the line blending did not permit measuring these values accurately. In the present work we adopted the aforementioned parameters from the NIST database.

The initial $V \sin i$ value has been estimated from the average value obtained from the first zero of the Fourier transforms (FT) of all neutral helium lines in the spectrum in the range 4000 Å to 5000 Å, adopting a quadratic limb-darkening law (Wade & Rucinski 1985) to determine the rotational broadening function (Gray 1992; Carroll 1933) as in our previous works (Levenhagen & Künzel 2011; Levenhagen & Leister 2004, 2006).

The stellar bolometric luminosity $\log L/L_\odot$, mass $M/M_\odot$, and age $\log \tau$ were estimated through interpolation in the evolutionary tracks of non-rotating stars calculated by Schaller et al. (1992), taking $Z = 0.02$. In this procedure we used a similar geometrical construction proposed in Myakutin & Piskunov (1995) to interpolate the solution in the evolutionary tracks. The final set of parameters, neglecting the effects of gravity darkening, are shown in Table 3. Figure 2 presents line fittings at Hβ, Hγ, Hδ, He I 4471 Å, and Mg II 4481 Å line transitions.

3.1. Estimation of parameters at the stellar pole and equator

Main sequence stars belonging to B and O spectral types present high mean rotation velocities, with equatorial speeds as high as a few hundred km s^{-1} and can no longer be treated as spherically symmetrical. A rigid star subjected to a high rotational velocity field flattens in its polar regions and enlarges at the equator (Collins 1963; Roxburgh et al. 1965), so the stellar poles receive more energy by surface unit area than the equator. Inside the star, the radiative flux exists because of the temperature gradient, and the last one is due to a pressure gradient among the stellar layers. As the star must be in hydrostatic equilibrium, the pressure gradient is determined by the gravity $\left(\frac{dP}{dr} = -g\right)$ so the outgoing flux is proportional to gravity as stated by the Von Zeipel's theorem. The gravitational acceleration is evaluated through the Roche approximation of the surface potential, which in turn takes the potential due to the total mass distribution and the rotational potential into account, neglecting multipole terms in the Legendre polynomial expansion due to the non-spherical mass distribution:

$$\Phi_{\rm eff} = -\frac{GM}{R(\theta)} - \frac{1}{2}\Omega^2 R(\theta)^2 \sin^2\theta \tag{1}$$

where θ is the angle between the rotation axis and the radial vector $\boldsymbol{R}$, where $R(\theta = 0°) = R_{\rm pole}$ and $R(\theta = 90°) = R_{\rm eq}$. The norm of the gravity vector $\boldsymbol{g} = -\boldsymbol{\nabla}\Phi$ is

$$\begin{aligned} g &= \sqrt{\left(\frac{\partial\phi}{\partial R}\right)^2 + \left(\frac{\partial\phi}{\partial\theta}\right)^2} \\ &= \left[\left(\frac{GM}{R^2} - \Omega^2 R\sin^2\theta\right)^2 + \left(\Omega^4 R^2 \sin^2\theta\cos^2\theta\right)\right]^{1/2} \end{aligned} \tag{2}$$

where the radius R is evaluated at all latitudes through numerical interpolation.

In this work model spectra were also evaluated by taking the gravity darkening effects into account, with the purpose of estimating the aspect angle i. The values of fundamental parameters corrected for gravitational darkening were inferred by directly comparing the observed spectra with synthetic models built up from non-LTE stellar atmosphere models of rotationally distorted stars. In this procedure, we assumed (1) a stellar mass distribution equivalent to that of a Roche model; (2) rigid rotation; and (3) the stellar core unaffected by rotation; i.e., bolometric luminosity is the same as for a non-rotating star.

We divided the stellar surface into a mesh of about 200 000 slabs (both hemispheres, including the non-visible side), each one with its own colatitude-dependent photospheric parameters $T(\theta)$ and $\log\ g\ (\theta)$, according to the relation

Table 3. Number of energy levels and radiative transitions adopted in synthesis procedures.

Parameters based on non-rotating models		Parameters based on rotating models	
$T_{\rm eff}$	22 000 ± 300 K	$T_{\rm pole}$	23 264 ± 300 K
log g	3.65 ± 0.11 dex	$T_{\rm eq}$	19 104 ± 300 K
$V \sin i$	130 ± 15 km s^{-1}	$R_{\rm pole}$	5.96 ± 0.1 $R_\odot$
log τ	7.37 ± 0.08 yr	$R_{\rm eq}$	7.04 ± 0.1 $R_\odot$
log $L/L_\odot$	3.93 ± 0.07	log $g_{\rm pole}$	3.83 ± 0.11 dex
$M/M_\odot$	8.9 ± 0.1	log $g_{\rm eq}$	3.48 ± 0.11 dex
$12 + \log\left(\frac{He}{H}\right)$	10.87 ± 0.03 dex	$V/V_{\rm c}$	0.68 ± 0.04
$12 + \log\left(\frac{Mg}{H}\right)$	7.57 ± 0.02 dex	i	30° ± 2°
$\xi_{\rm micro}$	6.4 ± 0.2 km s^{-1}		

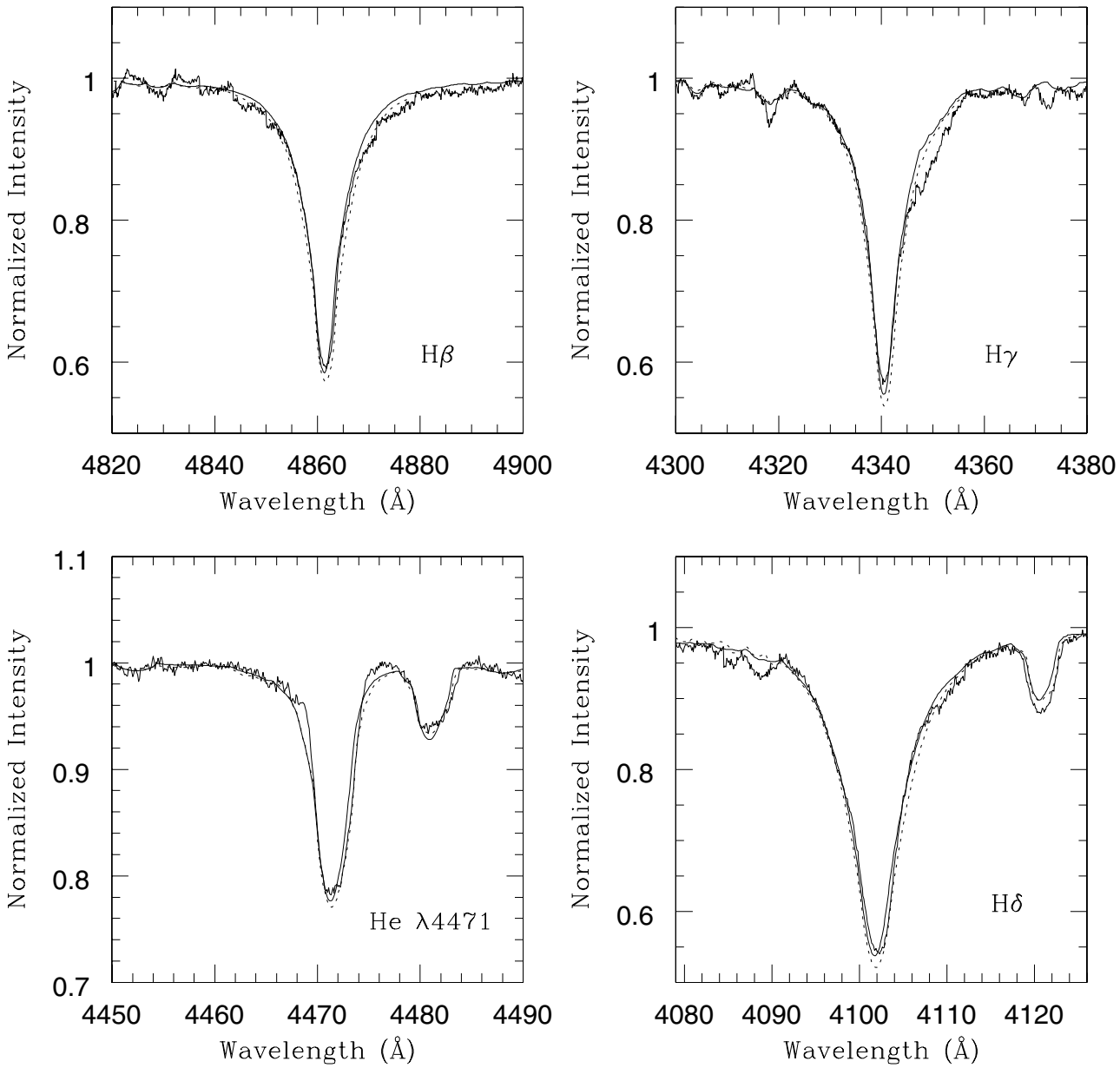

Fig. 2. Best fitting of Hβ (*upper left panel*), Hγ (*upper right*), He I 4471 Å and Mg II 4481 Å (*bottom left*), and Hδ (*bottom right*) line profiles with a large set of non-LTE models taking into account the gravitational darkening effects (full lines) and without the assumption of rotational distortion due to gravity darkening (dots).

(Lovekin et al. 2006; von Zeipel 1924a,b):

$$T(\theta) = T_p \left(\frac{g(\theta)}{g_p}\right)^{0.25}. \quad (3)$$

Each element area is written as

$$\mathrm{d}\boldsymbol{A} = \left(\frac{\mathrm{d}\boldsymbol{R}}{\mathrm{d}\theta} \times \frac{\mathrm{d}\boldsymbol{R}}{\mathrm{d}\phi}\right) \mathrm{d}\theta \mathrm{d}\phi \quad (4)$$

or

$$\mathrm{d}A = R^2 \sin\theta \mathrm{d}\theta \mathrm{d}\phi \sqrt{1 + \left(\frac{\Delta R}{R}\right)^2}. \quad (5)$$

Only specific intensities coming from visible elements of the grid are integrated, resulting in the final line profile.

To constrain the parameters at the pole and equator, we built up a large set of stellar models with varying parameters $M/M_\odot$, log g, log $L/L_\odot$, i, and V/V_c and performed a minimization with the Downhill-Simplex algorithm (Nelder & Mead 1965). The resulting corrected line profiles (Hβ, Hγ, Hδ, He I 4471 + Mg II 4481 Å) are shown in Fig. 2, and the parameters of the gravity-darkened model are given in Table 3.

4. Time series analyses

The search for line profile variations (lpv's) in He I, Fe II and Si II of λ Pav has been addressed with the *Cleanest* algorithm, which is well-suited for non-equispaced time series (Foster 1996).

Iteratively, this method subtracts the respective strongest signal and its aliases, as determined by the window function, from the input signal. The process continues until there are no more statistically significant peaks in the residuals. V/R ratio time series of He I, Fe II and Si II line profiles have been also built up and the data has been processed with the *Cleanest* algorithm. Radial velocities for each spectroscopic transition have been evaluated from MCT/LNA and ESO's spectra by cross-correlation of λ Pav line profiles with radial velocity standard stars obtained during the same observing runs (using the IRAF's task *fxcor*). Time series analyses of radial velocities have been performed again with the *Cleanest* algorithm.

All the stellar spectra have been arranged into 3 sets. Set 1 concerns to spectra observed from 1999 Oct. 18 to 1999 Oct. 24. Set 2 are the spectra obtained from 2000 Oct. 17 to 2000 Oct. 20, plus 2001 Apr. 02 to 2001 Aug. 03. Set 3 comprises all the observational seasons together.

Each data set has been divided into several time series centred on the transition wavelengths listed in Table 4, with wavelength spacing steps of 0.1 Å (Fig. 1, upper left panel). All series were analysed with a frequency search compatible for the limitations on the window sample to be studied. The lpv signals with highest confidence levels detected with Cleanest in all data sets concerning He I, Fe II, Mg II, and Si II lines are shown in Table 4. Confidence levels and periodograms pertaining to all signals detected in lpv's at He I 6678 Å are shown in Fig. 3. The window spectrum corresponding to all the observational campaigns (set 3) is presented in Fig. 4 and reveals a clear correlation of the data with a sampling signal of 1 c/d.

From the estimation of atmosphere parameters $T_{\rm eff}$ = 22 000 K and log g = 3.65 dex, the bolometric luminosity and stellar mass were derived through the interpolation in the internal structure models (Schaller 1992) and are respectively log $L/L_\odot$ = 3.93 or $L = 3.27 \times 10^{30}$ W and $M/M_\odot$ = 8.9, compatible with a stellar radius $R/R_\odot$ = 6.32. From the best fit of models affected by the stellar rotation, we derive an aspect angle $i = 30°$, which is near the value estimated by Frémat et al. (2005) for this object (27.3° ± 1.1°). Provided the projected rotation velocity is $V \sin i$ = 130 km s^{-1}, the associated corotation frequency ν = 0.81 c/d is inferred, which in turn has been detected in several time series of line profiles, in V/R times series of He I, Fe II, Si II, and also V_R (Table 4) and labelled ν_3. The apparent linkage of ν_3 with rotation depends on the existence of a corotating signature such as a stellar spot or even the orbital timescale of ejected material, but this discussion is beyond the scope of this publication, so we refer to it simply as a corotation frequency. This value is near the corotating signature of ω CMa modelled by Maintz et al. (2003), which presents similar values of fundamental parameters $T_{\rm eff}$ and log g, and by extension a resembling radius.

The signal ν_1, which was detected at several transitions (Table 4) in all datasets, was found here by performing the analysis of data for which its biggest contiguous stream extends over almost one week, which places its periodic/secular or even irregular character beyond the scope of the data, hence needing further investigation. It also appears in the V/R Balmer lines wings time series analyses of the period 1999 Oct. 18 to 1999 Oct. 24 and radial velocity time series, which would be compatible with the observed mid-term variations in Balmer line wings (Fig. 1, bottom left and right). Later on, the star reached an almost quiescent phase in 2000, and again entered an active phase in 2001. Recently, Groh et al. (2007) pointed out an X-ray source near λ Pav and suggest there is a binary companion as a possible scenario. Again, the natural limitations in our time sample, made it impossible to ascribe a signal related to binarity, and

Table 4. Resulting LPV, V/R and V_R signals from the time series analyses of all profiles.

LPV's	ν_1 (c/d)	ν_2 (c/d)	ν_3 (c/d)	ν_4 (c/d)	ν_5 (c/d)
Fe II 5169 Å	0.20	0.56	0.82	1.58	2.20
He I 4009 Å	0.18	0.50	0.80	1.55	2.23
He I 4026 Å	0.18	0.51	—	1.65	—
He I 4121 Å	—	0.59	0.80	1.67	2.37
He I 4144 Å	0.16	—	0.85	—	—
He I 4388 Å	0.15	0.52	0.86	1.60	2.15
He I 4471 Å	—	0.55	0.79	1.62	—
He I 4922 Å	0.13	0.51	0.79	—	2.28
He I 6678 Å	0.20	0.54	0.80	1.61	2.06
Mg II 4481 Å	0.12	0.50	—	1.54	—
Si II 4131 Å	0.16	—	0.83	1.61	—
V/R					
Fe II 5169 Å	0.15	—	—	—	2.14
He I 4009 Å	0.18	0.46	—	—	—
He I 4026 Å	0.20	0.45	—	—	—
He I 4121 Å	0.18	0.43	—	—	—
He I 4144 Å	0.16	0.44	—	—	—
He I 4388 Å	0.17	—	0.81	1.64	—
He I 4471 Å	—	—	0.87	—	2.31
He I 4922 Å	0.16	0.45	—	1.69	—
He I 6678 Å	0.20	0.44	0.81	—	—
Mg II 4481 Å	0.22	0.51	—	1.65	—
Si II 4131 Å	0.16	—	0.80	—	—
V_R					
Fe II 5169 Å	0.22	—	—	1.61	—
He I 4009 Å	0.20	0.40	0.80	—	2.20
He I 4026 Å	0.16	0.41	0.83	1.59	—
He I 4121 Å	0.17	0.52	—	1.63	—
He I 4144 Å	0.15	0.48	0.88	1.68	—
He I 4388 Å	0.16	—	—	—	2.23
He I 4471 Å	0.18	0.55	0.80	1.67	—
He I 4922 Å	—	0.41	—	—	—
He I 6678 Å	0.17	0.50	—	1.66	—
Mg II 4481 Å	0.16	0.45	—	—	—
Si II 4131 Å	0.18	0.46	—	—	—

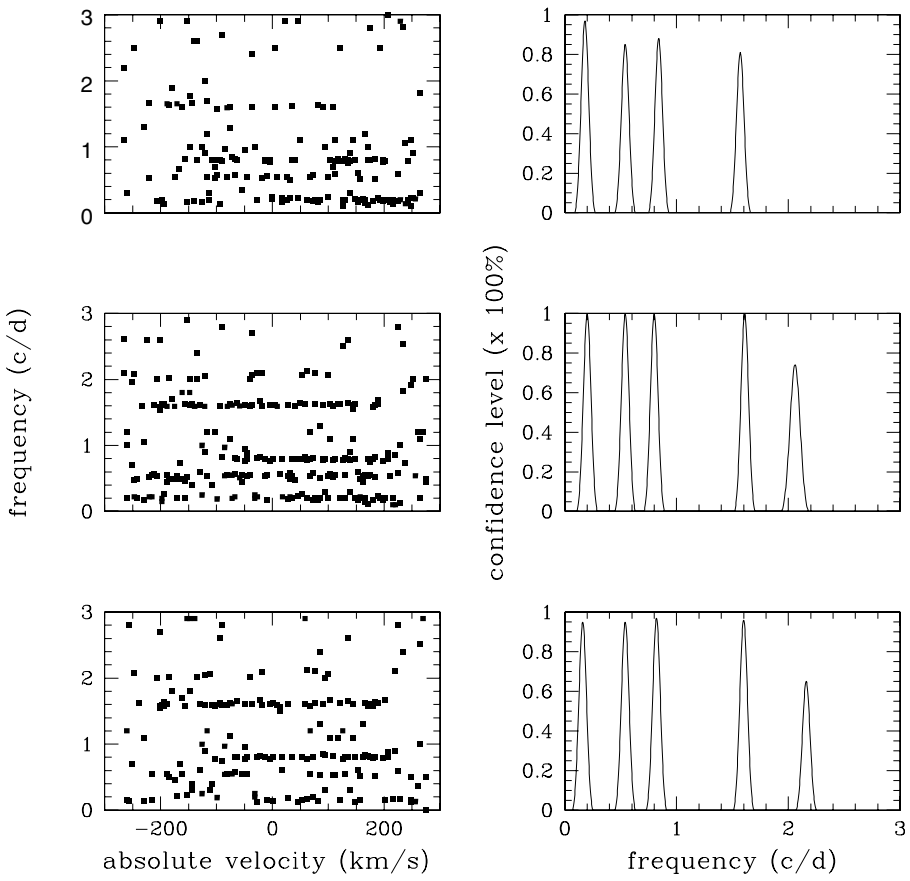

Fig. 3. Confidence levels and periodograms of signals detected in He I 6678 Å line profiles. (*Upper panels*) Periodogram (*left*) and confidence levels (*right*) for data set 2 from 2000 Oct. 17 to 2001 Aug. 03. (*Middle panels*) The same, but for data set 1, from 1999 Oct. 18 to 1999 Oct. 24. (*Bottom panels*) Diagrams for all the observational seasons.

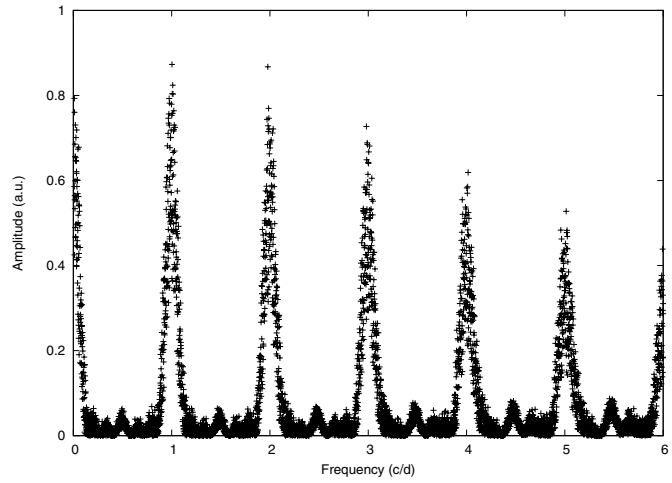

Fig. 4. Window spectrum concerning all observational campaigns.

also it is unlikely that ν_1 arise from that since it would lead to a very short period, which is typical of Algol-type stars. Despite insufficient time coverage to confirm the ν_1 signal, it was also detected by other authors (Koen & Eyer 2002) from photometric studies based on the Hipparcos data (ESA 1997), and we think it is possibly an alias of the corotating frequency ν_3, as $\nu_3 = 1 - \nu_1$.

The signal ν_4 is shown by earlier photometric studies (Hubert & Floquet 1998), appearing intensely in He I, Fe II, and Si II line profiles (Table 4, Figs. 3 and 5) and also in V/R and V_R. Similar frequency value has also been found in other Be stars, such as η Cen (Levenhagen et al. 2003; Štefl et al. 1995), DU Eri (Hubert & Floquet 1998), o And (Sareyan et al. 1998), and 28 Cyg (Balona 1995), among others. The spectroscopic residuals, optimized for phase coverage of ν_4 signal (Fig. 5), seem to trace the features expected for a low-degree g-mode. We regard it as a non-radial pulsation frequency (nrp), where ν_2 could be taken as its possible alias since $\nu_4 = 1 + \nu_2$.

The signal ν_5 appears only marginally in sets 1 and 3, with a confidence level between 60% and 80%, and does not appear in set 2. It could perhaps be related to a combination of signals ν_2 and ν_4, but due to its weakness it will not be considered in our analysis.

5. Conclusions

In this work we report the optical observations of the Be star λ Pavonis (HD 173948) spanning 1999 to 2001. Even though it is a bright ($B = 4.064$ mag) and hot object, it has never been the subject of customary asteroseismological studies in the past decades, and even its time-varying emission episodes have been reported sporadically.

Time series analyses (TSA) of line profile variations (lpv), radial velocities, and V/R ratios on He I line profiles ($\lambda\lambda$ 4026, 4121, 4144, 4388, 4471, 4922, 6678 Å), Fe II λ 5169 Å, and Si II λ 4131 Å were performed and pointed out the presence of only four signals: $\nu_1 = 0.17 \pm 0.02$ c/d, $\nu_2 = 0.49 \pm 0.05$ c/d, $\nu_3 = 0.82 \pm 0.03$ c/d, and $\nu_4 = 1.63 \pm 0.04$ c/d. Due to the limitations of the time sampling, the physical nature of the ν_1 signal, if produced by circumstellar phenomena or binarity, cannot be established in this work, so only the fact of the variability itself with a weekly time scale can be concluded. On the other hand,

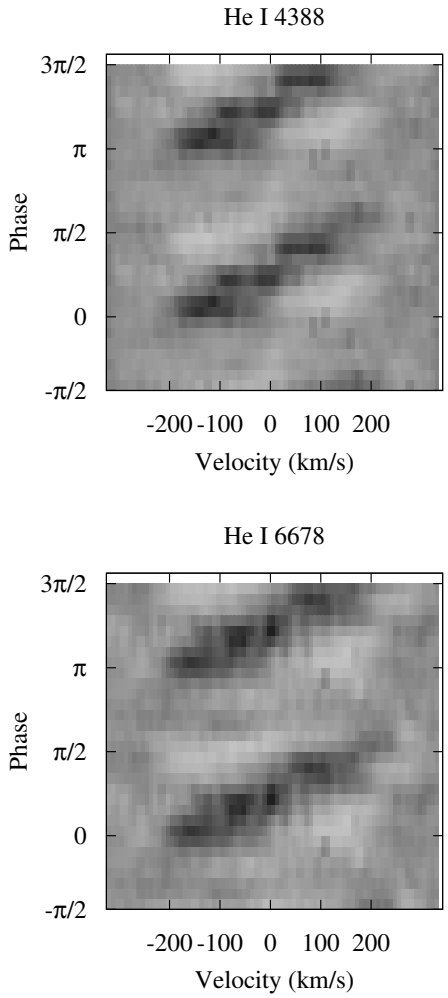

Fig. 5. Phased residuals of λ Pav, centered at He I 6678 Å and He I 4388 Å, with period ν_4.

the wings of the Hα line profiles exhibited strong variabilities, observed in the period Oct./18 to Oct./24/1999, with a period of about six days, reinforcing the presence of this signal. Koen & Eyer (2002) also reported a signal 0.16 c/d (or 6.18 days) in their analyses of the Hipparcos data. Also, some authors (Groh et al. 2007) argue that this object is in fact a binary star, as has been proposed recently for other Be stars such as Achernar (Kervella et al. 2008). On the other hand, Eggleton & Tokovinin (2008) flag the star as a single object, and Lefèvre et al. (2009) point to it as an irregular variable star. If the object is a binary system, then one would expect sinusoidal variations in radial velocity. Actually, from the radial velocity time series we also detected a signal ν_1, but if we interpret this variability as due to a stellar companion, it would give rise to the shortest orbital period known for a classical Be star, as the other known B binaries with such short periods are supposed to be Algol-type (interacting) stars. To confirm the binarity scenario, long-term photometric/spectroscopic observations are still needed.

The physical properties of the photosphere were also investigated, and the fundamental parameters of the photosphere ($T_{\rm eff}$ = 22 000 ± 300 K, log g = 3.65 ± 0.11, $V \sin i$ = 130 ± 15 km s^{-1}) were derived from the spectra. The fitting of non-LTE models taken into account for gravity darkening revealed the star has an aspect angle i = 30° ± 2° and a rotation rate of $V/V_{\rm c} \sim 0.68 \pm 0.04$, resulting in a theoretical rotation frequency of about 0.81 c/d.

From all the TSA performed with line profiles, radial velocity, and V/R, we detected ν_3 = 0.82 ± 0.03 c/d. We think this disturbance is most probably to be assigned to a corotating signature such as the orbital timescale of ejected material, even though the uncertainties in the stellar parameters also make this signal possibly related to the same retrograde mode suggested for many other Be stars (Rivinius et al. 2003).

It should be stressed, however, that the estimates of the aspect angle i and the rotation rate $V/V_{\rm c}$, and consequently the corotation frequency, depend strongly on the photospheric input parameters, and their errors should only be viewed as formal errors related to the fitting process. For example, a recent study of masses and luminosities of OB stars based on Hipparcos/Simbad and 2MASS photometry (Hohle et al. 2010) leads to $M/M_\odot$ = 12.47 and $L/L_\odot$ = 31 032, which is quite different from our parameters. These values imply $V/V_{\rm c} \sim 0.80$ and i = 40°, and a different value for the corotating signature is achieved, $\nu_{\rm corot} \sim 0.6$ c/d. Also, the mass and luminosity proposed by these authors depend on accurate knowledge of other relevant parameters, such as the galactic extinction, distance, and the extinction due to a circumstellar environment, provided the object is a Be star.

The ν_4 frequency has been reported by earlier spectroscopic studies of λ Pav (Hubert & Floquet 1998) and re-appears with strong intensity in our data sample. The sampling, optimized for phase coverage of this signal, seems to trace the features expected for an $\ell = |m| = 2$ g-mode, as seen in the He I 4833, 6678 Å residuals (Fig. 5). Such a signal is a "recidivist" one, as has also been detected in other Be stars such as κ CMa (Rivinius et al. 2003), η Cen (Levenhagen et al. 2003; Štefl et al. 1995), DU Eri (Hubert & Floquet 1998), o And (Sareyan et al. 1998), and 28 Cyg (Balona 1995), and usually attributed to NRP. Following this canonical interpretation, we assume the signal ν_4 would arise from NRPs, with ν_3 associated to the period of ejected material orbiting the star, where ν_1 and ν_2 are possibly their aliases. Other possible scenarios still pop up because $\nu_4 = 2 \times \nu_3$. Assuming the parameters hinted as in by Hohle et al. (2010) to be correct, then the derived corotating signature $\nu_{\rm corot} \sim 0.6$ c/d could be regarded as the detected signal ν_2, within the error bars, ν_3 would be the pulsation frequency with ν_1 as its alias, and ν_4 could be viewed as the first harmonic of the pulsation frequency ν_3. Regardless of the pictures presented, the behaviour of the line profiles of λ Pav is quite complex, and any conclusive scenario deserves further investigation involving observations in other spectral ranges, such as X-rays and long-term photometry to constrain binarity, as well as long-term, high-resolution spectroscopic observations aiming to confirm lpv signals.

Acknowledgements. The authors are grateful for the valuable comments and suggestions made by an anonymous referee. Financial support for this research has been granted by the Brazilian Agencies FAPESP (*Fundação de Amparo à Pesquisa do Estado de São Paulo*) through grants No. 04/14256-8 and 2010/06814-4, and CNPq (*Conselho Nacional de Desenvolvimento Cientifico e Tecnológico*) through grant 307095/2008-8. The ESO observations were performed through CNPq grant 1998/10138-8.

References

Ando, H. 1983, A&A, 35, 343
Ando, H. 1986, A&A, 163, 97
Asplund, M., Grevesse, N., & Sauval, A. J. 2005, in Cosmic Abundances as Records of Stellar Evolution and Nucleosynthesis, ed. F. N. Bash, & T. G. Barnes, ASP Conf. Ser., 336, 25

Balona, L. A. 1995, MNRAS, 277, 1547
Carroll, J. A. 1933, MNRAS, 93, 478
Chen, H., Ringuelet, A., Sahade, J., & Kondo, Y. 1989, ApJ, 347, 1082
Collins, G. W., II. 1963, ApJ, 138, 1134
Cunto, W., Mendoza, C., Ochsenbein, F., & Zeipen, C. J. 1993, A&A, 275, L25
Eggleton, P. P., & Tokovinin, A. A. 2008, MNRAS, 389, 869
ESA 1997, The Hipparcos and Tycho Catalogues, ESA SP-120
Foster, G. 1996, AJ, 111, 541
Frémat, Y., Zorec, J., Hubert, A. M., & Floquet, M. 2005, A&A, 440, 305
Gray, D. F. 1992, in The observations and analysis of stellar photospheres (Cambridge Univ. Press), 368
Groh, J. H., Damineli, A., & Jablonski, F. 2007, A&A, 465, 993
Hohle, M. M., Neuhäuser, R., & Schutz, B. F. 2010, Astron. Nachr., 331, 349
Hubeny, I. 1988, Comput. Phys. Comm., 52, 103
Hubeny, I., Hummer, D. G., & Lanz, T. 1994, A&A, 282, 151
Hubert, A. M., & Floquet, M. 1998, A&A, 335, 565
Johnson, H. L., & Mitchell, R. I. 1975, RMxAA, 1, 299
Kambe, E., Ando, H., & Hirata, R. 1993, A&A, 273, 435
Kervella, P., Domiciano de Souza, A., & Bendjoya, Ph. 2008, A&A, 484, 13
Koen, C., & Eyer, L. 2002, MNRAS, 331, 45
Lefèvre, L., Marchenko, S. V., Moffat, A. F. J., & Acker, A. 2009, A&A, 507, 1141
Levenhagen, R. S., & Künzel, R. 2011, NewA, 16, 307
Levenhagen, R. S., & Leister, N. V. 2004, AJ, 127, 1176
Levenhagen, R. S., & Leister, N. V. 2006, MNRAS, 371, 252
Levenhagen, R. S., Leister, N. V., Zorec, J., et al. 2003, A&A, 400, 599
Lovekin, C. C., Deupree, R. G., & Short, C. I. 2006, ApJ, 643, 460
Maintz, M., Rivinius, Th., Štefl, S., et al. 2003, A&A, 411, 181
Martin, W. C., Sugar, J., Musgrove, A., Wiese, W. L., & Fuhr, J. R. 1999, NIST Atomic Spectra Database (Gaithersburg: NIST)
Mennickent, R. E. 1991, A&AS, 88, 1
Moujtahid, A., Zorec, J., & Hubert, A. M. 1999, A&A, 349, 151
Myakutin, V. I., & Piskunov, A. Eh. 1995, AZh, 72, 358
Nelder, J. A., & Mead, R. 1965, Comput. J., 7, 308
Porter, J. M., & Rivinius, Th. 2003, PASP, 115, 1153
Rivinius, Th., Štefl, S., & Baade, D. 1999, A&A, 348, 831
Rivinius, Th., Baade, D., & Štefl, S. 2003, A&A, 411, 229
Roxburgh, I. W., Griffith, J. S., & Sweet, P. A. 1965, Z. Astrophys., 61, 203
Sahade, J., Rovira, M., Ringuelet, A. E., Kondo, Y., & Cidale, L. 1988, ApJ, 327, 335
Sareyan, J. P., Gonzalez-Bedolla, S., Guerrero, G., et al. 1998, A&A, 332, 155
Schaller, G., Schaerer, D., Meynet, G., et al. 1992, A&AS, 96, 269
Štefl, S., Baade, D., Harmanec, P., & Balona, L. A. 1995, A&A, 294, 135
Townsend, R. H. D., Owocki, S. P., & Howarth, I. D. 2004, MNRAS, 350, 189
Vinicius, M. M. F., Zorec, J., Leister, N. V., & Levenhagen, R. S. 2006, A&A, 446, 643
von Zeipel, H. 1924a, MNRAS, 84, 665
von Zeipel, H. 1924b, MNRAS, 84, 684
Wade, R. A., & Rucinski, S. M. 1985, A&A, 60, 471
Zorec, J., Frémat, Y., & Cidale, L. 2005, A&A, 441, 235